Research Article

Molecular Imaging
Volume 17: 1-5

DOI: 10.1177/1536012118788636
journals.sagepub.com/home/mix
SAGE

Acute Ketamine Infusion in Rat Does Not Affect In Vivo [^{11}C]ABP688 Binding to Metabotropic Glutamate Receptor Subtype 5

Lauren Kosten[1], Jeroen Verhaeghe[1], Leonie wyffels[1,2], Sigrid Stroobants[1,2], and Steven Staelens[1]

Abstract

Detecting changes in metabotropic glutamate receptor 5 (mGluR5) availability through molecular imaging with the positron emission tomography (PET) tracer [^{11}C]ABP688 is valuable for studying dysfunctional glutamate transmission associated with neuropsychiatric disorders. Using an infusion protocol in rats, we visualized the acute effect of subanesthetic doses of ketamine on mGluR5 in rat brain. Ketamine is an N-methyl-D-aspartate (NMDA) receptor antagonist known to increase glutamate release. Imaging was performed with a high-affinity PET ligand [^{11}C]ABP688, a negative allosteric modulator of mGluR5. Binding did not change significantly from baseline to ketamine in any region, thereby confirming previous literature with other NMDA receptor antagonists in rodents. Hence, in rats, we could not reproduce the findings in a human setup showing significant decreases in the [^{11}C]ABP688 binding after a ketamine bolus followed by ketamine infusion. Species differences may have contributed to the different findings in the present study of rats. In conclusion, we could not confirm in rats that endogenous glutamate increases by ketamine infusion are reflected in [^{11}C]ABP688 binding decreases as was previously shown for humans.

Keywords

glutamate, molecular imaging, mGluR5, ketamine

Introduction

Detecting changes in receptor availability at the metabotropic glutamate receptor 5 (mGluR5) with the positron emission tomography (PET) allosteric antagonist, [^{11}C]ABP688, is valuable for studying dysfunctional glutamate transmission associated with psychiatric illnesses such as schizophrenia,[1] depression,[2] and obsessive compulsive disorder.[3]

Studies with pharmacological challenges to increase endogenous glutamate levels attempt to provide insight into glutamate receptor availability. Both N-acetyl-cysteine and MK801 are studied in literature because of their glutamate-increasing properties.[4,5] Whereas ketamine is sometimes the anesthetic of choice in these studies,[4] ketamine in itself also has effects on glutamate transmission in the brain. In literature, first evidence was provided that ketamine administration decreases binding of the high-affinity PET ligand [^{11}C]ABP688 in vivo in humans.[6] These results suggest that [^{11}C]ABP688 (a negative allosteric modulator of mGluR5) binding is sensitive to ketamine-induced effects, a known N-methyl-D-aspartate (NMDA) receptor antagonist increasing glutamate release[7] through disturbed gamma-aminobutyric acid (GABA) transmission of inhibitory neurons, as shown in Figure 1A. The ionotropic NMDA receptor is ligand gated requiring glutamate binding and voltage dependent as illustrated in Figure 1B. Ketamine binds noncompetitively to the receptor. Our objective is to image the acute effect of subanesthetic doses of ketamine using a mimicked infusion protocol.

[1] Molecular Imaging Center Antwerp, University of Antwerp, Antwerp, Belgium
[2] Department of Nuclear Medicine, University Hospital Antwerp, Antwerp, Belgium

Submitted: 19/01/2018. Revised: 18/05/2018. Accepted: 15/06/2018.

Corresponding Author:
Steven Staelens, Faculty of Medicine and Health Sciences, Campus Drie Eiken, Room UC.059, Universiteitsplein 1–2610 Wilrijk, Belgium.
Email: steven.staelens@uantwerpen.be

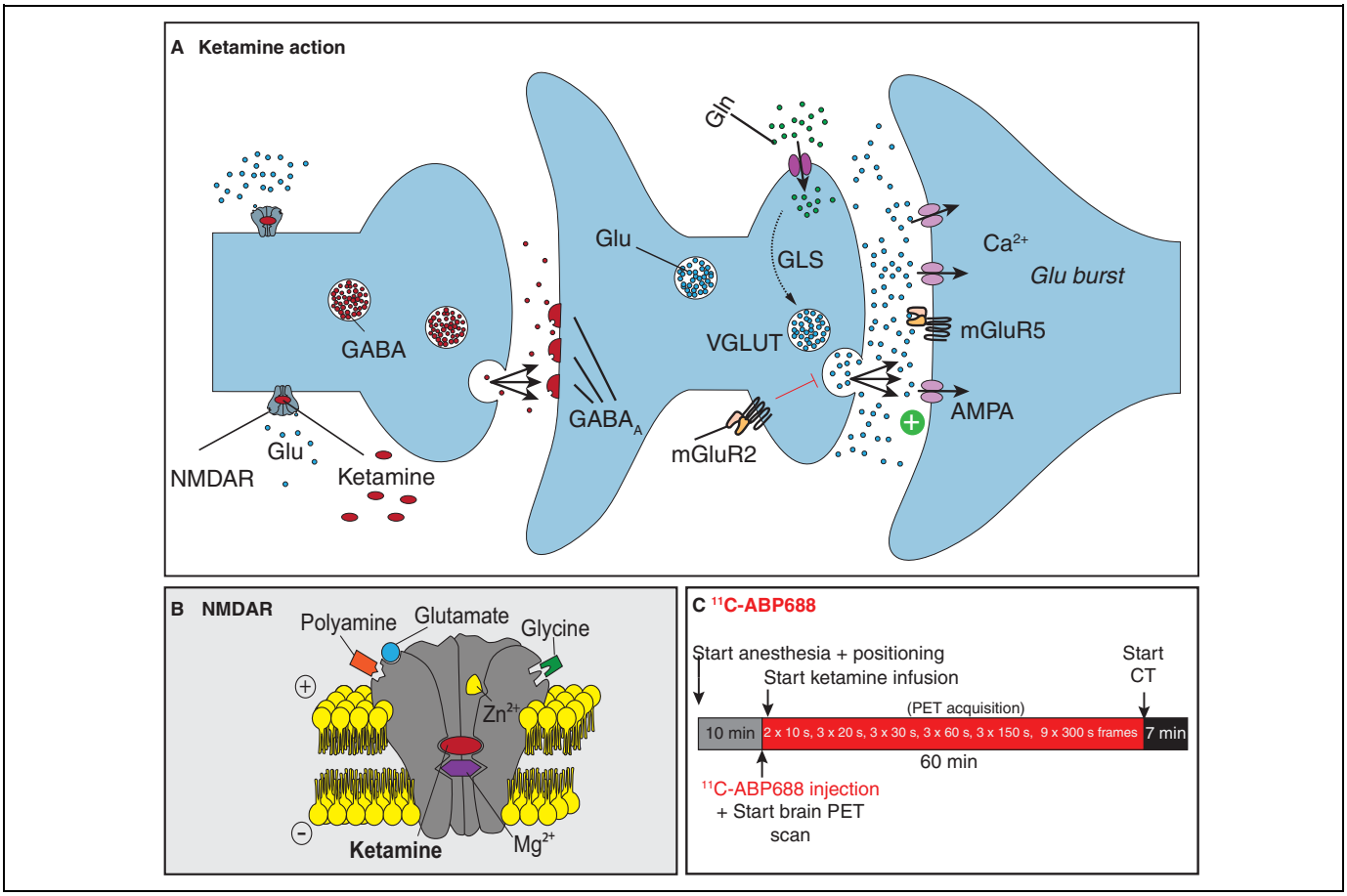

Figure 1. Experimental procedures. A, Mechanism of action for ketamine. GABA transmission of inhibitory neurons is disturbed, leading to increased glutamate release. B, Detail of the ionotropic NMDA receptor which is (i) ligand-gated requiring glutamate to bind with coactivation of D-serine or glycine and (ii) voltage-dependent through channel blocks by extracellular Zn^{2+} and Mg^{2+} ions. Ketamine is a noncompetitive antagonist by binding in the open channel and at an allosteric site. C, Ketamine was continuously infused during the scan. The final dose of 30 mg/kg is reached at the middle of the last frame from a 60-minute dynamic acquisition of [11C]ABP688. After the positron emission tomography scan, a computed tomography scan is taken for attenuation correction. NMDA indicates N-methyl-D-aspartate.

Experimental Procedures

Male Sprague Dawley rats (n = 8; 385-525 g) underwent a baseline scan and a scan with ketamine administration on the same day under isoflurane anesthesia (mixture with medical oxygen 5% for induction and 1.5% maintenance). To control for diurnal variations between animals,[8] time between the baseline and challenge scans was kept consistent for all animals with an SD of only 18 minutes (an average of 3 hours and 24 minutes). All baseline scans started between 10:48 AM and 11:34 AM, whereas ketamine challenge scans started between 2:20 PM and 2:57 PM. For ketamine, a concentration of 30 mg/kg was chosen[9,10] as higher concentrations (40 mg/kg) are reported to show loss of excitation.[6,11,12] As ketamine is extremely rapidly eliminated, with a redistribution half-life of around 15 minutes,[6,13] we opted for an infusion paradigm as shown in Figure 1C, where ketamine was continuously infused via the tail vein during the scan. The final dose of 30 mg/kg is reached at the middle of the last frame from a 60-minute dynamic acquisition of [^{11}C]ABP688 (1.058 ± 0.176 mCi; 32.71 ± 10.44 GBq/μmol; <3 nmol/kg, intravenous).

Ketamine Blood Levels

We aim to reach at least 10 mg/kg in the brain, taking into account pharmacokinetic properties and tissue distribution of ketamine, and to validate that accurate blood levels of ketamine were achieved; a satellite group of n = 3 was infused at the same rate with ketamine as described above. Blood samples were taken at $t = 51.5$ minutes from start of the infusion, which corresponds to the middle of the last frame for the dynamic PET acquisitions. Ketamine levels were quantified with a forensic enzyme-linked immunosorbent assay kit (Neogen Europe, Ayr, United Kingdom).

Image Analysis

For quantitative analysis, small-animal PET images were reconstructed by use of 2-dimensional ordered-subset

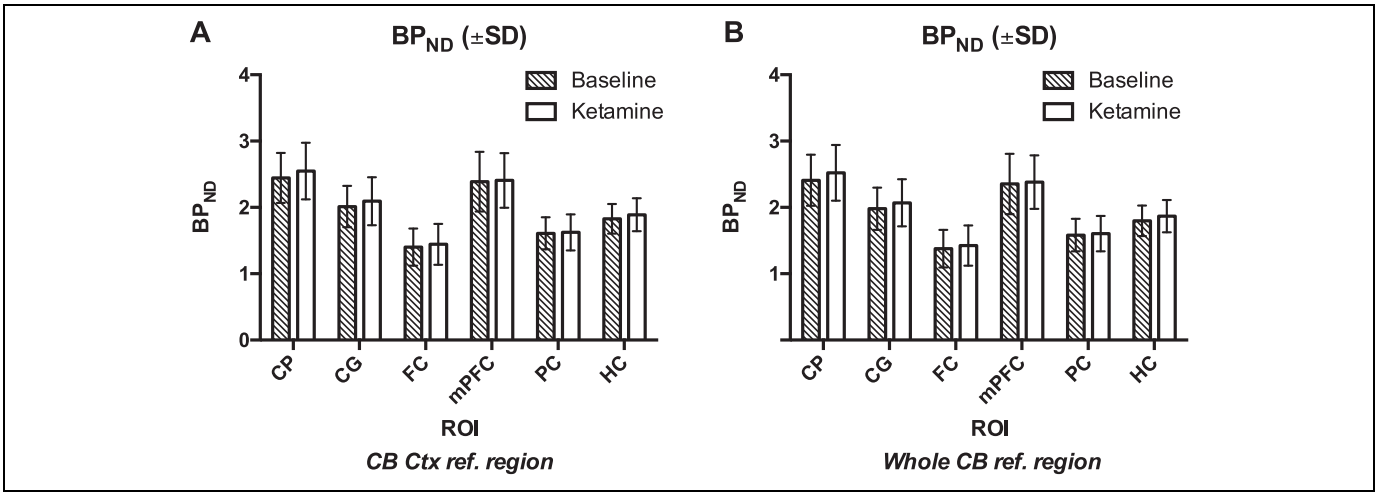

Figure 2. Nondisplaceable binding potential values for CG, FC, mPFC, PC, HC, and CP are shown after kinetic modeling using SRTM. A, The reference region for SRTM analysis was the cerebellar cortex. B, The reference region for SRTM analysis was the whole cerebellum. Mean ± SD. CG indicates cingulate cortex; CP, caudate putamen; FC, frontal cortex; HC, hippocampus; mPFC, medial prefrontal cortex; PC, parietal cortex; SRTM, simplified reference tissue model.

expectation maximization with 4 iterations and 16 subsets after Fourier rebinning. The PET images were reconstructed on a 128 × 128 × 159 grid with a pixel size of 0.776 × 0.776 × 0.776 mm. The reconstructed spatial resolution was about 1.4 mm at the center of the field of view (with filtered back-projection). Normalization, dead time correction, random subtraction, computed tomography–based attenuation, and single-scatter simulation scatter corrections were applied. For each dynamic acquisition, a static image corresponding to the time-averaged frames was spatially transformed through brain normalization with PMOD version 3.3 (PMOD Technologies, Zürich, Switzerland) to an in-house-developed [^{11}C]ABP688 template of the rat brain. Each frame in the dynamic sequence of individual scans was then transformed to the [^{11}C]ABP688 template space according to calculated transformation parameters. The time–activity curves for several volume of interests (VOIs) were extracted from the images. The nondisplaceable binding potential (BP_{ND}) of [^{11}C]ABP688 for the different VOIs was then calculated by use of simplified reference tissue model (SRTM) with the cerebellar cortex as a reference region,[14,15] as previous methods using the whole cerebellum possibly affects the results due to mGluR5 expression in the deep cerebellar nuclei.[16,17] Additionally, voxel-based statistical parametric mapping (SPM) analysis was performed using the SPM8 (Welcome Department of Cognitive Neurology, London, United Kingdom) within a one-way repeated-measures ANOVA design. The images were smoothed using a Gaussian filter (isotropic 1.5 mm full-width-at-half-maximum). An F-contrast, testing for any difference between the challenges, and T-contrasts, testing for both increased and decreased binding for ketamine infusion versus baseline, were defined. Voxels that passed the omnibus F test at a significance level of 0.05 (uncorrected) defined a mask for the subsequent post hoc T-contrasts. T-maps were thresholded at a significance level of 0.05 (uncorrected) with a cluster extent threshold of 125 voxels (1 mm^3).

Results

Ketamine Enzyme-Linked Immunosorbent Assay

Blood sample analysis measured blood levels of 2.34 ± 0.46 mg/kg in the blood at $t = 51.5$ minute. With a known ratio of about 6.5 to 1 for brain versus plasma[9,10,18], this corresponds to brain ketamine levels of approximately 15.22 ± 2.98 mg/kg.

Volume of Interest–Based Analysis

Nondisplaceable binding potential did not change significantly from baseline to ketamine in any region as shown in Figure 2A: +3.92 ± 5.97% in the cingulate cortex, +3.21 ± 10.56% in the frontal cortex, +1.48 ± 8.43% in the medial prefrontal cortex, +0.77 ± 5.23% in the parietal cortex, +3.46 ± 6.31% in the hippocampus, and +4.12 ± 5.24% in the caudate putamen (CP). When using SRTM to calculate BP_{ND} values with the whole cerebellum as reference region, also no significant differences were found (Figure 2B). Figure 3 illustrates the averaged PET images on a magnetic resonance (MR) template.

Voxel-Based SPM Analysis

The voxel-based SPM analysis revealed that ketamine infusion challenge did not induce significant changes in [^{11}C]ABP688 binding, when compared to baseline.

Discussion

In previous work by our group,[5] [11C]ABP-688 test–retest variability in rats without a ketamine any challenge was 2.0% ± 10.7% for the BP_{ND} in the CP as equally demonstrated in other studies with rats and also primates.[4,5,14] The nonsignificant variations we demonstrate with the current study of 4.12 ± 5.24% in the CP after a ketamine challenge are within

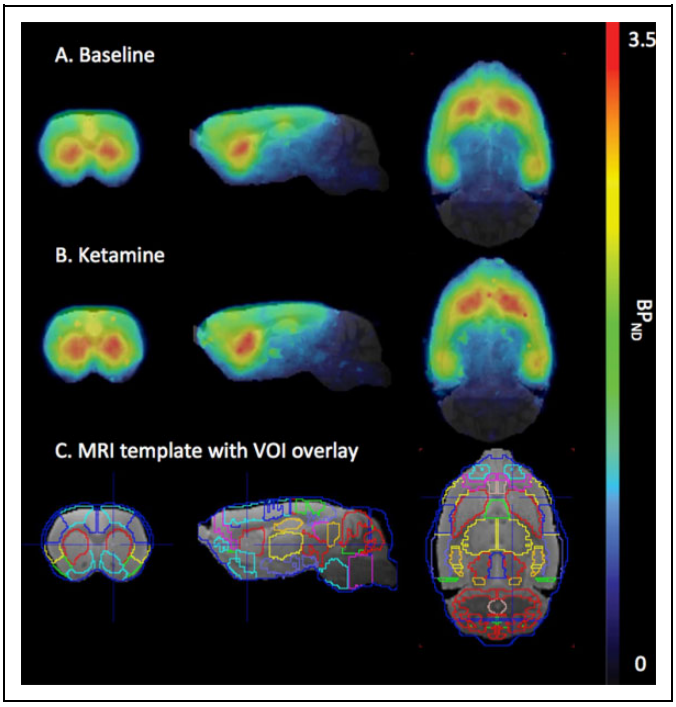

Figure 3. The PET images average BP_{ND}. A, Mean BP_{ND} PET images overlay on MR template for the baseline scan. B, Mean BP_{ND} PET images overlay on MR template for the ketamine challenge scan. C, Magnetic resonnace template with VOI overlay. Scale 0 to 3.5. BP_{ND} indicates nondisplaceable binding potential; PET, positron emission tomography; VOI, volume of interest

this test–retest variability and hence likely not attributable to the effects of ketamine. Our results on the net effect of ketamine on [^{11}C]ABP688 BP_{ND} in rats do not reflect the findings of DeLorenzo et al in a human setup,[6] showing decreases with high variation in the [^{11}C]ABP688 BP_{ND} after bolus of 0.23 mg/kg followed by infusion of 0.58 mg/kg ketamine, with 7 subjects experiencing <20% decrease in average volume of distribution (V_T) after ketamine infusion and 3 subjects experienced >40% decrease. In a later publication, the authors cite evidence suggesting glutamatergic regulation of the circadian cycles that might even cause underestimation of abovementioned ketamine effects.[8,19] A 2017 publication by Esterlis et al repeats the finding of reduced mGluR5 availability in humans following ketamine administration, as visualized with [^{11}C]ABP688 V_T.[20] This finding of decreased [^{11}C]ABP688 BP_{ND} would intuitively suggest direct competition for the binding place, yet DeLorenzo et al and Esterlis et al note that glutamate does not directly impact the binding of [^{11}C]ABP688 in a membrane preparation but it does lead to receptor internalization. The authors find that reduction persisted after 24 hours, possibly reflecting an imbalance between mGluR5 internalization and the rate of recycling to the cytoplasma membrane. Since it has been shown that the half-life of ketamine in rat brain is approximately 0.9 hours,[18,21] we opted for a higher infusion dose than DeLorenzo et al as the metabolism of ketamine in human brain is lower (half-life of $\sim$3 hours).[22]

On the other hand, with our data, we confirm previous results of Wyckhuys et al[5] and Sandiego et al[4] who also showed that [^{11}C]ABP688 BP_{ND} did not reflect changes in acute endogenous glutamate fluctuations in rat and rhesus monkey, respectively, with other NMDA antagonists. Species differences may have contributed to the different findings in the present study of rats versus the humans. Because this study was in anesthetized animals, there might possibly be an effect on glutamate release and binding, contributing to the difference in outcome between our study and in vivo awake human study by DeLorenzo et al.[6] First, as for the effects of volatile anesthetics on the results of the study, the influence of isoflurane anesthesia on glutamate binding has been assessed in literature.[10,23,24] It was concluded that isoflurane at clinically relevant levels does not have substantial effects on synaptosomal uptake, synaptic membrane binding, or transport of glutamate. Second, in vitro data[25] showed that isoflurane reduces both Ca^{2+}-independent and Ca^{2+}-dependent glutamate release, and another study suggested that volatile anesthetics such as isoflurane reduce the ratio of basal glutamate to GABA release, possibly contributing to a net depression of glutamatergic excitation.[26] Recently, however, Seidemann et al did an *in vivo* study on the influence of volatile anesthesia on glutamate release[27] in rats. Animals received anesthesia for 3 hours, yet at any of the individual time points during isoflurane anesthesia, glutamate release did not differ significantly. As a future solution to optimize translation between clinical and preclinical setups, our group is optimizing protocols for awake scanning as exemplified by Miranda et al,[28,29] an approach that has also been presented by Sandiego et al for nonhuman primate brain PET imaging for evaluation of $GABA_A$-benzodiazepine binding.[30]

Conclusions

We could not confirm in rats that endogenous glutamate changes by ketamine infusion are reflected in [^{11}C]ABP688 BP_{ND} changes as was previously shown for humans.

Acknowledgments

The authors are grateful to colleagues Caroline Berghmans and Philippe Joye of MICA, University of Antwerp, for their help with the scan acquisitions.

Declaration of Conflicting Interests

The author(s) declared no potential conflicts of interest with respect to the research, authorship, and/or publication of this article.

Funding

The author(s) received no financial support for the research, authorship, and/or publication of this article.

References

1. Poels EMP, Kegeles LS, Kantrowitz JT, et al. Imaging glutamate in schizophrenia: review of findings and implications for drug discovery. *Mol Psychiatry*. 2014;19:20–29.

2. Deschwanden A, Karolewicz B, Feyissa AM, et al. Reduced metabotropic glutamate receptor 5 density in major depression determined by [(11)C]ABP688 PET and postmortem study. *Am J Psychiatry*. 2011;168:727–734.
3. Akkus F, Terbeck S, Ametamey SM, et al. Metabotropic glutamate receptor 5 binding in patients with obsessive-compulsive disorder. *Int J Neuropsychopharmacol*. 2014;17(12):1915–1922.
4. Sandiego CM, Nabulsi N, Lin S-F, et al. Studies of the metabotropic glutamate receptor 5 radioligand [^{11}C]ABP688 with N-acetylcysteine challenge in rhesus monkeys. *Synapse*. 2013b; 67:489–501.
5. Wyckhuys T, Verhaeghe J, Wyffels L, et al. N-acetylcysteine- and MK-801-induced changes in glutamate levels do not affect in vivo binding of metabotropic glutamate 5 receptor radioligand 11C-ABP688 in rat brain. *J Nucl Med*. 2013;54(11):1–8.
6. DeLorenzo C, DellaGioia N, Bloch M, et al. In vivo ketamine-induced changes in [(11)C]ABP688 binding to metabotropic glutamate receptor subtype 5. *Biol Psychiatry*. 2015;77(3):266–275.
7. Moghaddam B, Adams B, Verma A, Daly D. Activation of glutamatergic neurotransmission by ketamine: a novel step in the pathway from NMDA receptor blockade to dopaminergic and cognitive disruptions associated with the prefrontal cortex. *J Neurosci*. 1997;17:2921–2927.
8. DeLorenzo C, Gallezot J-D, Gardus J, et al. In vivo variation in same-day estimates of metabotropic glutamate receptor subtype 5 binding using [11C]ABP688 and [18F]FPEB. *J Cereb Blood Flow Metab*. 2017;37(8):2716–2727.
9. Dedeurwaerdere S, Wintmolders C, Straetemans R, Pemberton D, Langlois X. Memantine-induced brain activation as a model for the rapid screening of potential novel antipsychotic compounds: exemplified by activity of an mGlu2/3 receptor agonist. *Psychopharmacology (Berl)*. 2011;214:505–514.
10. Duncan GE, Leipzig JN, Mailman RB, Lieberman JA. Differential effects of clozapine and haloperidol on ketamine-induced brain metabolic activation. *Brain Res*. 1998;812:65–75.
11. Miyamoto S, Leipzig JN, Lieberman JA, Duncan GE. Effects of ketamine, MK-801, and amphetamine on regional brain 2-deoxyglucose uptake in freely moving mice. *Neuropsychopharmacology*. 2000;22:400–412.
12. Wyckhuys T, Wyffels L, Langlois X, Schmidt M, Stroobants S, Staelens S. The [18F]FDG μPET readout of a brain activation model to evaluate the metabotropic glutamate receptor 2 positive allosteric modulator JNJ-42153605. *J Pharmacol Exp Ther*. 2014; 350:375–386.
13. Clements JA, Nimmo WS. Pharmacokinetics and analgesic effect of ketamine in man. *Br J Anaesth*. 1981;53:27–30.
14. Elmenhorst D, Aliaga A, Bauer A, Rosa-Neto P. Test-retest stability of cerebral mGluR$_5$ quantification using [^{11}C]ABP688 and positron emission tomography in rats. *Synapse*. 2012;66:552–560.
15. Rubins DJ, Melega WP, Lacan G, et al. Development and evaluation of an automated atlas-based image analysis method for microPET studies of the rat brain. *NeuroImage*. 2003;20: 2100–2118.
16. Daggett LP, Sacaan AI, Akong M, et al. Molecular and functional characterization of recombinant human metabotropic glutamate receptor subtype 5. *Neuropharmacology*. 1995; 34:871–886.
17. DeLorenzo C, Milak MS, Brennan KG, Kumar JSD, Mann JJ, Parsey RV. In vivo positron emission tomography imaging with [^{11}C]ABP688: binding variability and specificity for the metabotropic glutamate receptor subtype 5 in baboons. *Eur J Nucl Med Mol Imaging*. 2011;38:1083–1094.
18. Cohen ML, Chan SL, Way WL, Trevor AJ. Distribution in the brain and metabolism of ketamine in the rat after intravenous administration. *Anesthesiology*. 1973;39:370–376.
19. Elmenhorst D, Mertens K, Kroll T, et al. Circadian variation of metabotropic glutamate receptor 5 availability in the rat brain. *J Sleep Res*. 2016;25:754–761.
20. Esterlis I, DellaGioia N, Pietrzak RH, et al. Ketamine-induced reduction in mGluR5 availability is associated with an antidepressant response: an [(11)C]ABP688 and PET imaging study in depression. *Mol Psychiatry*. 2018;23(4):824–832.
21. Zou X, Patterson TA, Sadovova N, et al. Potential neurotoxicity of ketamine in the developing rat brain. *Toxicol Sci*. 2009;108: 149–158.
22. Li L, Vlisides PE. Ketamine: 50 years of modulating the mind. *Front Hum Neurosci*. 2016;10:612.
23. Dedeurwaerdere S, Wintmolders C, Vanhoof G, Langlois X. Patterns of brain glucose metabolism induced by phosphodiesterase 10A Inhibitors in the mouse: a potential translational biomarker. *J Pharmacol Exp Ther*. 2011; 339:210–217.
24. Westphalen RI, Hemmings HC. Effects of isoflurane and propofol on glutamate and GABA transporters in isolated cortical nerve terminals. *Anesthesiology*. 2003;98:364–372.
25. Larsen M, Grøndahl TO, Haugstad TS, Langmoen IA. The effect of the volatile anesthetic isoflurane on Ca(2+)-dependent glutamate release from rat cerebral cortex. *Brain Res*. 1994;663: 335–337.
26. Westphalen RI, Hemmings HC. Volatile anesthetic effects on glutamate versus GABA release from isolated rat cortical nerve terminals: basal release. *J Pharmacol Exp Ther*. 2006;316: 208–215.
27. Seidemann T, Spies C, Morgenstern R, Wernecke K-D, Netzhammer N. Influence of volatile anesthesia on the release of glutamate and other amino acids in the nucleus accumbens in a rat model of alcohol withdrawal: a pilot study. *PLoS One*. 2017;12: e0169017.
28. Miranda A, Staelens S, Stroobants S, Verhaeghe J. Fast and accurate rat head motion tracking with point sources for awake brain PET. *IEEE Trans Med Imaging*. 2017;36:1573–1582.
29. Miranda A, Staelens S, Stroobants S, Verhaeghe J. Markerless rat head motion tracking using structured light for brain PET imaging of unrestrained awake small animals. *Phys Med Biol*. 2017;62: 1744–1758.
30. Sandiego CM, Jin X, Mulnix T, et al. Awake nonhuman primate brain PET imaging with minimal head restraint: evaluation of GABAA-benzodiazepine binding with 11C-flumazenil in awake and anesthetized animals. *J Nucl Med*. 2013;54:1962–1968.